Korean Journal of Chemical Engineering
https://doi.org/10.1007/s11814-024-00260-9

REVIEW ARTICLE (INVITED ONLY)

Electrochemical Monitoring for Molten Salt Pyroprocessing of Spent Nuclear Fuel: A Review

Wonseok Yang[1] · Richard I. Foster[1] · Jihun Kim[2] · Sungyeol Choi[1,2,3]

Received: 2 April 2024 / Revised: 19 July 2024 / Accepted: 13 August 2024

Abstract

Pyroprocessing holds the key to unlocking a more sustainable future for nuclear energy by handling various types of spent nuclear fuel (SNFs) and reducing radioactive waste volumes. This review examines the role of electrochemical monitoring in molten salt pyroprocessing of SNFs, emphasizing its importance in enhancing process efficiency and nonproliferation. Challenges associated with the monitoring of multi-element environments, flow environments, and sensor stability are discussed. The review suggests that integrating sensor technology with artificial intelligence could lead to significant advancements in the field.

Keywords Nuclear energy · Actinide · Fission product · Reprocessing · Recycling · Circular economy

Introduction

Nuclear energy, recognized as a sustainable power source, addresses energy security and climate change concerns [1]. Recent advancements in small modular reactors (SMRs) have expanded nuclear technology applications beyond electricity generation to include high-temperature output non-electric sectors, such as hydrogen production, synthetic chemicals, and metal refining [2, 3]. This broadened scope has intensified the focus on nuclear power. Nevertheless, the management of spent nuclear fuel (SNF)—nuclear fuel that is no longer economically or technically viable for energy generation due to diminished fissile material (i.e. ^{235}U) and increased neutron poison content (e.g. ^{135}Xe, ^{149}Sm, ^{157}Gd, etc.)—poses significant challenges.

SNF still contains substantial quantities of valuable actinides, such as, Pu, and minor actinides (MA) which could be reused as fuel. Also, it contains highly radioactive Fission Products (FP) that require careful management and appropriate final disposal [4–7]. Pyroprocessing offers a potential solution by recycling SNF through a high-temperature electrochemical process with the aim of separating U as well as transuranic elements (TRU), Pu and MA, from FPs [4, 8–11].

Operating between 400 and 1000 °C, pyroprocessing utilizes molten salt electrolytes to separate actinides from FPs and other undesirable elements. As shown in Fig. 1, its stages include (1) head-end process (decladding, voloxidation), (2) electrolytic reduction, (3) electrorefining, and (4) electrowinning. Contrasting with the PUREX process, which uses organic solvents for chemical separation, pyroprocessing is carried out in molten salts at high temperatures. This difference gives several advantages to pyroprocessing over PUREX. One of the significant advantages of pyroprocessing is its versatility in handling various fuel types even with higher burn-up rates and various fuel types, including those from fast reactors. Pyroprocessing's high chloride concentration without a water medium minimizes the risk of criticality accidents [8, 9, 12–14]. The process does not produce pure Pu, making the resulting materials less attractive for proliferation [8, 9, 11, 15]. The elimination of organic solvents also reduces the environmental and safety hazards associated with chemical processing [11]. Nonetheless, it is important to recognize that advanced hydrometallurgical processes, while not yet industrialized at scale, also offer significant advantages, such as not producing pure Pu, as discussed by

✉ Sungyeol Choi
choisys7@snu.ac.kr

[1] Nuclear Research Institute for Future Technology and Policy, Seoul National University, Seoul 08826, Republic of Korea

[2] Department of Nuclear Engineering, Seoul National University, 1 Gwanak-ro, Gwanak-gu, Seoul 08826, Republic of Korea

[3] Institute of Engineering Research, Seoul National University, Seoul 08826, Republic of Korea

Published online: 28 August 2024

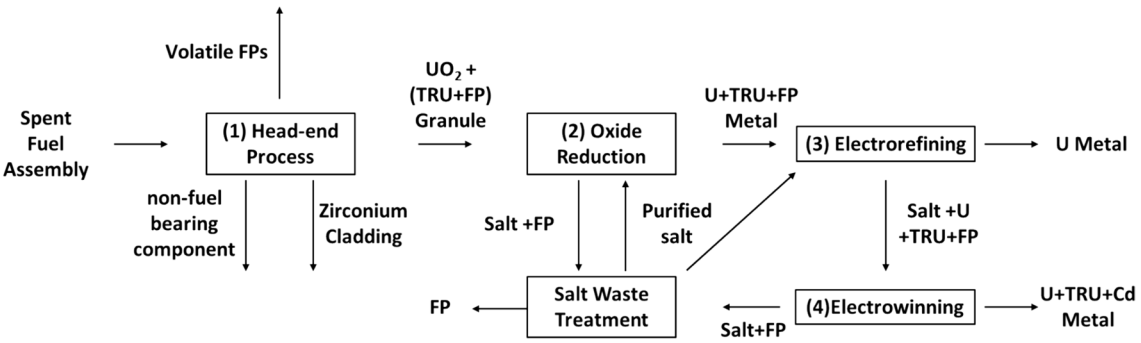

Fig. 1 Schematic flowsheet of the pyroprocessing

Taylor et al.[16]. The benefits of pyroprocessing also open up possibilities for resolving legacy waste issues that plague the nuclear industry such as bespoke one-off fuel types developed for research reactors or graphitic wastes [17–20].

As with most chemical processes, real-time monitoring of the composition and properties of the system [21–23], in this case, the molten salts, is crucial for the safe and efficient operation of pyroprocessing [24–26]. This information is used for process control, optimization, and the early detection and prevention of problems [27]. Electrochemical monitoring enables the direct and continuous measurement of key parameters such as concentration of ions, and salt potential, providing valuable data for the optimization of the pyroprocessing operations [28–32]. For example, oxygen concentration is a key aspect of optimizing the oxide reduction process in pyroprocessing [27], because it is related to the reaction rate [33] and anode protection [34]. The advantages of electrochemical monitoring include rapid and real-time measurement capabilities, suitability across a wide electrochemical window of molten salts, and compatibility with remote handling operations necessary for worker safety. [28–30, 35, 36]. While there is no requirement for calibration standards, performance in high radiation environments has been observed to be generally robust, particularly with adequate shielding; however, direct evidence of complete unaffectedness is limited. Therefore, electrochemical monitoring methods have been developed to monitor U [29, 30, 37, 38], TRU elements [29], FPs [31], and oxygen concentration [39–42]. However, further development is required for applications in environments with high temperatures and corrosiveness, especially over long-term operation cycles, and where a variety of nuclear species are present [43]. This includes advancing the durability and stability of monitoring equipment to withstand the harsh operational conditions and improving the ability to accurately measure multielements simultaneously [37].

The objective of this review is to provide a comprehensive overview of the necessity, development status, and suggestions for future research of electrochemical sensors designed for utilization in pyroprocessing, a critical technology in nuclear fuel reprocessing. The review will cover the description of processes using molten salts in pyroprocessing, the purpose of monitoring in pyroprocessing, major elements in pyroprocessing, current electrochemical sensor technology applicable to molten salt systems, and suggestions for future research. This review highlights the current challenges and outlines future directions for the development of advanced electrochemical sensors, including the suggested integration of machine learning-coupled electrochemical sensors [44, 45]. The advancement is expected to focus on enhancing (1) material compatibility, (2) improving measurement accuracy, and (3) integrating sensor technology with process control systems; thereby contributing to the optimization and expansion of pyroprocessing capabilities.

Composition of Spent Nuclear Fuel

Commercially operating reactors include light-water moderated reactors (LWRs), heavy-water moderated reactors (PHWRs), graphite moderated reactors, and fast breeder reactors. Among these, LWRs are the most widely used and constructed, thus this paper will primarily focus on SNF from LWRs, unless specified otherwise.

Natural U predominantly consists of fertile ^{238}U (99.3%) and fissile ^{235}U (0.7%), along with trace amounts of other isotopes such as ^{233}U, ^{234}U, and ^{236}U. To use U as fuel for LWRs, it should be enriched up to 2–5% of ^{235}U [46]. When going through the process of nuclear fission, the composition of the nuclear fuel changes. The nuclear fission process alters the composition of the fuel, with the specific composition of SNF depending on the initial fuel type, chemical composition, level of enrichment, neutron energy spectrum, and "burn-up"—the thermal energy generated per unit mass of fuel [47]. Fuel is classified as "spent" once it loses efficiency for nuclear fission, primarily due to a reduction in fissile material and an accumulation of neutron-absorbing FPs.

Table 1 shows the typical changes in LWR fuel composition from enriched fresh fuel to SNF at a burn-up of 46 GWD/tU.

Handling SNF is challenging due to its high heat generation and radioactivity. The radioactivity of SNF at typical burn-up increases to the order of 10^{17} Bq/MT compared to fresh fuel because of the radioactive decay of the elements inside of the fuel; particularly the short- and intermediate-lived radioisotopes. For the first 100 years after removal from a reactor core, the radioactivity of the SNF is dominated by FPs emitting beta and gamma rays. Thereafter, it is dominated by the actinides undergoing alpha decay.

Strategies for managing SNF include direct disposal in deep geological repositories (DGRs) without recycling, and reprocessing to separate usable nuclear materials (U and TRUs) from wastes (FPs) [4–7]. The purpose of direct disposal in a DGR is for the isolation of SNFs from the biosphere until the radiotoxicity of the SNFs decays enough. Reprocessing seeks to efficiently use U and other actinides while reducing waste volume and radiotoxicity.

Historically, few countries have decided to engage in reprocessing their SNF: China, France, India, Japan, Netherlands, Russia and U.K [15]. Among these, the only countries that currently operate commercial scale reprocessing facilities are France and Russia, with the U.K. choosing to close their Magnox and Thorp reprocessing plants in 2022 and 2018, respectively [16, 17], and the startup of the Rokkasho-Mura plant in Japan facing perpetual delays. A major reason inhibiting the widespread use of reprocessing is the concern about nuclear proliferation [15]. The aqueous reprocessing process PUREX, which is commercially available, can separate pure Pu from the spent nuclear fuel which enhances the nuclear proliferation risk. However, pyro-processing, which is being actively researched as an alternative to PUREX, uses molten salts. It produces a mixed ingot of U, Pu, and MA which can lower nuclear proliferation risk. To convert the TRU-U ingot from pyroprocessing into weapons-grade material, an additional processing step, such as using a covert PUREX plant, would be required, making the process more complex and easier to detect [15].

Table 1 The chemical composition of 4 wt% enriched LWR fresh fuel and 46 GWD/tU burnup spent nuclear fuel [126]

Element/isotope		Fresh fuel composition (wt%)	Spent fuel composition (wt%)
U	^{235}U	4.00	0.67
	^{236}U	Trace	0.50
	^{238}U	96.00	93.06
Pu		–	1.68
Minor actinides[a]		–	0.10
Fission products[b]		–	4.00

[a]Np, Am, Cm

[b]Transition metals, lanthanides (e.g. Sm, Gd, Eu), long lived radioisotopes (e.g. ^{90}Sr, ^{137}Cs, ^{99}Tc, ^{129}I)

Main Steps of Pyroprocessing

Pyroprocessing technology, initially developed for treating metallic fuel, has expanded to include recycling of SNF, such as oxide fuel from Pressurized Water Reactors (PWRs) [8]. This review primarily considers pyroprocessing for oxide fuel, given that PWRs are predominant in Korea and globally. Pyroprocessing aims to recycle SNF by separating valuable materials such as U and TRUs from SNF, thereby reducing the volume and toxicity of nuclear waste and contributing to a sustainable nuclear fuel cycle. The process involves several key stages: (1) head-end process (disassembly, rod extraction, cutting, and decladding, oxide feed fabrication, off-gas treatment process), (2) oxide reduction process, (3) electrorefining process, (4) electrowinning process, and (5) waste treatment process [9]. Oxide reduction, electrorefining, and electrowinning are all electrochemical processes that utilize molten salt as a solvent and an electrolyte with high radiation resistance.

Head-End Process

The head-end process (Fig. 2) is the initial series of steps preparing SNF for recycling and waste minimization, transforming the spent fuel assembly into a form suitable for further processing like oxide reduction and electrorefining. The key objectives and methods involved include follows [9]:

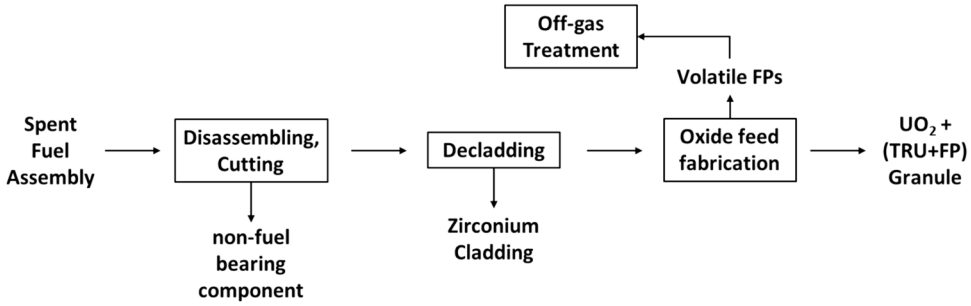

Fig. 2 Schematic flowsheet of the head-end process in pyroprocessing

Disassembling, Rod Extraction, and Cutting Process: This stage involves disassembling spent fuel assemblies to extract individual fuel rods. The rods are then mechanically cut into shorter segments suitable for decladding. This process is critical for breaking down the fuel assemblies into manageable pieces for further processing. Utilizing tele-operated manipulator systems ensures precision and safety due to the high radioactivity of SNF, enhancing the efficiency of subsequent processing steps by preparing the fuel in a more accessible form.

Decladding Process: It aims to remove the metal cladding encasing the fuel material, achieved through mechanical means or oxidative methods. The choice of method depends on factors like fuel burn-up rates and the desired efficiency of material recovery. This step is crucial for exposing the fuel material for further processing while ensuring valuable materials are not lost in the cladding [9].

Oxide Feed Fabrication Process: Following decladding, the fuel material is processed to create a suitable feed for the oxide reduction step. This may involve converting the fuel into powders or pellets that have specific characteristics, such as a porous structure for rapid reduction or a dense form to prevent contamination by salt carryover [9]. The goal is to prepare the fuel in a form that maximizes the efficiency of subsequent electrochemical processes [48]. The processed SNF (UO_2 + TRUs + FPs) is then placed in a cathode basket for the oxide reduction step in LiCl-Li_2O molten salt.

Off-gas Treatment Process: This step is concerned with treating fission gases released during the head-end process. The treatment aims to capture volatile (Kr, Xe, ^{14}C, ^{3}H) and semi-volatile fission products (Cs, I, Tc, Ru, Mo, Rh, etc.), preventing their release into the environment [49]. This step is crucial for environmental protection and for recovering valuable or hazardous materials contained in the gas form [9, 10, 50].

Molten Salt Process: Oxide Reduction

The oxide reduction process aims to convert spent oxide fuel into metallic form, facilitating further processing and recycling (Fig. 3). This process uses a molten salt electrolyte, typically LiCl-Li_2O, which serves as the medium for the electrochemical reduction of spent nuclear fuel oxides. Electrodes play a vital role in the process, with the spent oxide fuel acting as cathodes where the reduction occurs, and Pt or carbon based materials [51, 52], serving as anodes. The process reactions involve the transfer of electrons to oxide fuels, reducing it to its metallic form, while oxygen ions are transferred to anodes, completing the circuit (Fig. 4).

Cathode : $M_xO_y + 2ye^- \rightarrow xM(\text{actinide}) + yO^{2-}$,

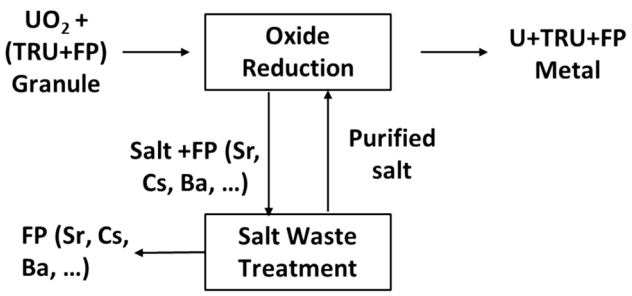

Fig. 3 Schematic flowsheet of the oxide reduction process in pyroprocessing

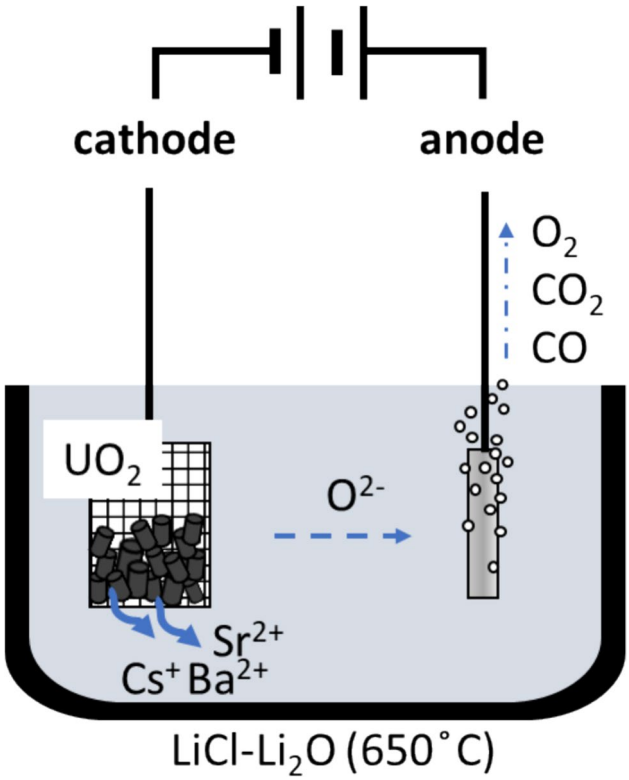

Fig. 4 Schematic diagram of the oxide reduction cell

Anode : $2O^{2-} \rightarrow O_2(g) + 4e^-$ at Pt anode,

$C + O^{2-} \rightarrow CO(g) + 2e^-$ at graphite anode,

$C + 2O^{2-} \rightarrow CO_2(g) + 4e^-$ at graphite anode.

The molten salt electrolyte not only facilitates these reactions but also acts as a medium for dissolving certain FPs (Cs, Ba, Sr), thereby separating them from the fuel [53–56]. This step is crucial for reducing the volume and heat load of the SNF, making it easier to handle and process further. The

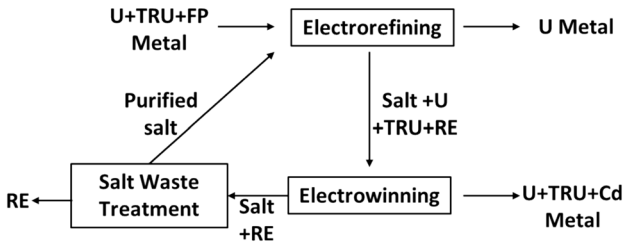

Fig. 5 Schematic flowsheet of the electrorefining and electrowinning process in pyroprocessing

development of efficient electrode designs and the optimization of salt composition are ongoing challenges in enhancing the efficiency and scalability of the oxide reduction process in pyroprocessing [33, 57, 58].

Molten Salt Process: Electrorefining

The objective of electrorefining in pyroprocessing is to extract purified U from the metallic form of SNF (Fig. 5). This purification process is essential for recycling these materials into new fuel, significantly reducing waste and the need for fresh U mining [59]. Typically, a LiCl–KCl eutectic serves as the electrolyte in this process, dissolving actinide chlorides to enable the selective deposition of U at the solid cathode. Meanwhile, TRUs and REs are either retained in the electrolyte or collected at the anode, achieved through meticulous control of the cell's electrochemical potential [56, 60–62].

The anode is where the spent metallic fuel is introduced, and dissolution occurs, releasing U and other actinides into the molten salt. The cathode is typically made from a stable, inert material, such as Mo [63–65], Fe [64, 65], graphite [66], stainless steel (Grade-304) [67], and tungsten [67], where U is deposited in a pure form. The anode material can also be chosen for its scraping characteristics [66, 67]. The process reactions involve the oxidation of metallic U at the anode to form U chloride, which then migrates through the molten salt to be reduced back to metallic U at the cathode (Fig. 6).

$$\text{Anode}: \ \mathrm{U} \rightarrow \mathrm{U}^{3+} + 3\mathrm{e}^{-},$$

$$\mathrm{M(actinide\ and\ fission\ products)} \rightarrow \mathrm{M}^{x+} + \mathrm{xe}^{-},$$

$$\text{Cathode}: \mathrm{U}^{3+} + 3\mathrm{e}^{-} \rightarrow \mathrm{U}.$$

Through electrorefining, not only is U efficiently recovered, but the separation of REs and actinides is also achieved, contributing to a closed fuel cycle and reducing the long-term radiotoxicity and heat load of nuclear waste.

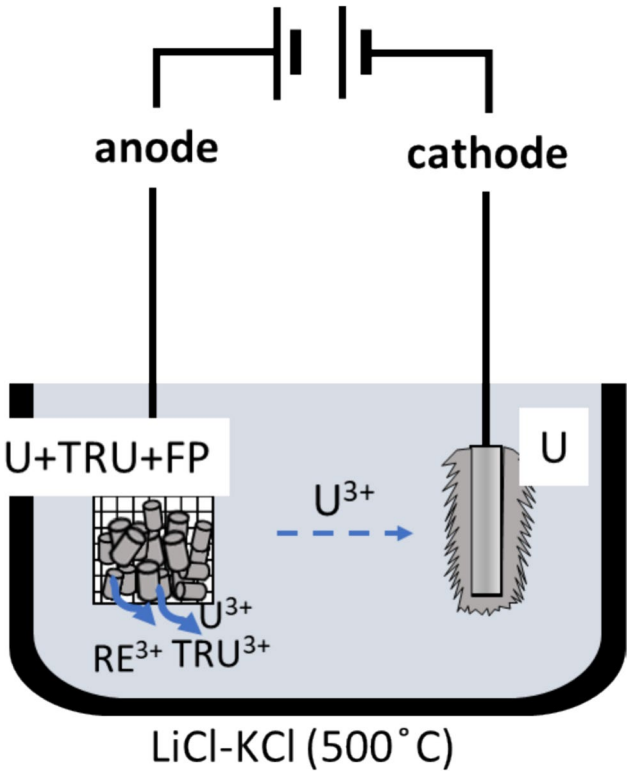

Fig. 6 Schematic diagram of electrorefining cell

The ongoing development of this technology focuses on improving the efficiency of U recovery and the purity of the product (without undesired TRU), ensuring that recycled fuel meets the necessary standards for re-use in reactors [55, 68–70].

Molten Salt Process: Electrowinning

Electrowinning follows electrorefining in the pyroprocessing sequence in order to recover valuable metals, primarily U and TRUs, from the spent electrolyte. As depicted in Fig. 6, the majority of U is already recovered during the electrorefining step. The electrowinning process is then applied to the molten salt electrolyte, which still contains residual U and TRUs, by changing the cathode to a liquid cadmium cathode (LCC) [9]. In electrowinning, the objective is to co-deposit the U and TRUs on LCC from the molten salt, which contains the dissolved metals [71, 72]. This process further minimizes waste and enables the recycling of all usable materials from SNF. Electrodes in electrowinning are uniquely configured to facilitate the deposition of metals on LCC. Recent studies are exploring the use of liquid bismuth (Bi) as well as cadmium (Cd) electrodes as cathode materials in the electrowinning step of pyroprocessing, showing promising alternative methodologies for metal recovery [73–77]. The research explored the use of liquid

Bi electrodes due to their lower melting point and potential for reduced toxicity compared to Cd, with the added potential for enhanced separation efficiency of lanthanides and actinide [77]. For instance, Sohn et al. investigated the spatial distribution of $CeBi_2$ within Bi-Ce alloys under various conditions to explore density-based separations between intermetallic compounds of actinides (An) and lanthanides (Ln) in used molten salt from pyroprocessing [77]. Further research should focus on utilizing density-based methods within liquid Bi metals to achieve low toxicity and high separation efficiency of actinides and lanthanides.

The anodes are generally made from inert materials that do not participate in the reaction, while the cathode is a pool of liquid metal such as Cd and Bi, which selectively accumulates U and TRUs from the electrolyte for proliferation resistance. The process reactions involve the reduction of metal ions from the molten salt onto a liquid metal cathode, where they form intermetallic compounds or dissolve into Cd or Bi. Table 2 shows the formal potentials of U, Pu, and Np at Mo and liquid metal cathode, respectively, and the activity coefficients for the intermetallic compounds. U has a much higher activity coefficient compared to Pu and Np, which makes it harder to form intermetallic compounds resulting in more negative formal potential than at the Mo cathode. Pu and Np both have low activity coefficients, which makes it easier for them to form intermetallic compounds, resulting in more positive formal potential than at the Mo cathode. As a result, the formal potentials of U and TRUs become much closer at the liquid metal cathode than at the Mo cathode. By applying voltage using the LCC, the combined intermetallic compound can be formed rather than the pure forms. At the anode, when an inert anode is used, chlorine gas is produced (Fig. 7) [78].

$$\text{Cathode}: U^{3+} + 3e^{-} \rightarrow U\,(\text{Cd}),$$

$$TRU^{3+} + 3e^{-} \rightarrow TRU\,(\text{Cd}),$$

$$\text{Anode}: 2Cl^{-} \rightarrow Cl_2 + 2e^{-}.$$

Electrowinning's capacity to distinguish TRUs from REs allows for the recycling of these elements into new reactor fuel, playing a crucial role in reducing high-level waste volumes and advancing nuclear power sustainability by closing the fuel cycle. Future advancements in molten salt compositions and electrode configurations are expected to increase the selectivity and efficiency of the electrowinning process [79]. The challenges in electrowinning include optimizing the process to maximize recovery rates, minimize impurities, and ensure the efficient separation of actinides from REs.

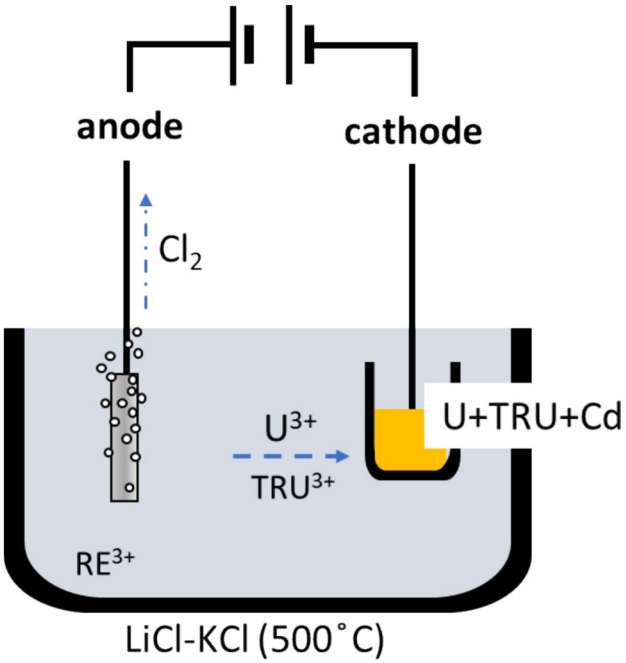

Fig. 7 Schematic diagram of electrowinning cell

Purpose of Electrochemical Monitoring in Pyroprocessing

Process Efficiency

The primary goal of real-time electrochemical monitoring in pyroprocessing is to enhance process efficiency. Monitoring allows for the adjustment of processes in response to the changing conditions of the molten salt medium, directly impacting the effectiveness of each pyroprocessing stage. By

Table 2 Formal potentials of U, Pu, Np at Mo, liquid Cd, and liquid Bi vs. Ag^{+}/Ag (1 wt%) and their activities in LiCl–KCl eutectic molten salts at 773K

	$E^{0'}$ (V) at Mo [127]	$E^{0'}$ (V) at liquid Cd [127]	Activity at liquid Cd [5]	$E^{0'}$ (V) at liquid Bi	Activity at liquid Bi[128]
U	−1.248	−1.310	7.5×10	−0.970 [127]	2.7×10^{-5}
Pu	−1.506	−1.345	1.4×10^{-4}	−1.080 [129]	4.5×10^{-10}
Np	−1.485	−1.376	8.2×10^{-3}	−1.066 [130]	4.0×10^{-8}

fine-tuning operational parameters, electrochemical monitoring plays a direct role in optimizing the efficiency of critical stages, including oxide reduction, electrorefining, and electrowinning.

In the oxide reduction stage, the concentration of O^{2-} ions is critical to the anode reaction [34]. At low O^{2-} concentrations, Pt dissolution occurs as Pt is converted to Pt^{2+} ions, releasing electrons. Conversely, high O^{2-} concentrations lead to Pt corrosion, forming Li_2PtO_3 through the reaction with Li ions and electrons. The concentration of FPs like Cs and Sr can increase during oxide reduction process [54]. They influence O^{2-} concentration, which affects the efficiency of the oxide reduction process [53].

$$Pt \rightarrow Pt^{2+} + 2e^{-},$$

$$Pt + 2Li^{+} + 3O^{2-} \rightarrow Li_2PtO_3 + 2e^{-}.$$

In the electrorefining stage, the focus is on extracting purified uranium from SNF's metallic form. The salt composition, including the concentrations of U and Pu, is directly related to the current density and, consequently, the deposition rate [80]. Pu can be deposited on the solid electrode, affecting the purity of the recovered U, at low concentrations of U ion [62, 81]. Lastly, the salt composition can determine the time to progression to the electrowinning with optimum efficiency. During electrowinning, U, TRU, and rare earth elements (REE) are recovered from the salt transferred from the electrorefining process. The composition of the salt and the metal composition in cadmium are crucial parameters. The current density, influenced by both the salt and metal compositions, dictates the efficiency of metal recovery [60].

Nonproliferation

Electrochemical monitoring plays a critical role in the nonproliferation aspect of pyroprocessing by monitoring the concentration of nuclear materials. Nuclear material accounting activities are carried out to establish the quantities of nuclear material present within defined areas [82]. Real-time accounting presents challenges, such as the inhomogeneity of the salt and the variation in the concentration of fissile materials near the anode and cathode during electrorefining [83]. The near-anode concentration of fissile material, such as Pu and U, tends to increase, while it decreases near the cathode, posing a challenge for accurate accounting and inventory control. Monitoring the concentrations of these materials in the molten salt and combining with computational simulation is vital for maintaining an accurate account of nuclear materials. Anomaly detection is another critical aspect, where monitoring sensor readings for unexpected changes in salt composition or redox potentials can indicate attempts at material diversion [84]. Such real-time monitoring capabilities are essential for promptly identifying and addressing potential nonproliferation risks, thereby ensuring the secure and compliant operation of pyroprocessing facilities.

Major Elements in Pyroprocessing

As an input of pyroprocessing, SNF is comprised of a complex mix of materials, including U, TRUs, along with a plethora of FPs. The composition of SNF depends on operation conditions. U is the predominant element in SNF, serving as the primary fuel used in nuclear reactors. TRUs such as Pu, Np, Am, and Cm are generated within the nuclear reactor through neutron capture and beta-decay processes starting from U. These TRUs are of particular interest in pyroprocessing due to their long half-lives and potential for reuse in nuclear reactors. During the fission process, U atoms split to produce a range of other elements, including rare earth elements (La, Ce, Nd, etc.), Cs, Sr, Zr, and noble metals. Table 3 gives summary of this section. The electrochemical properties of these elements are well-detailed in Zhang's review [85].

In pyroprocessing, the actinides—specifically U and Pu, alongside Np, Am, and Cm—are the primary elements of interest. The emphasis on U and Pu is due to their abundant presence in SNF and as fuel in nuclear power plants [5]. Monitoring these elements in real-time within the molten salt facilitates optimal control of electrorefining and electrowinning processes, ensuring the product meets purity specifications. Furthermore, from a nonproliferation standpoint, precise accountability of fissile materials, especially Pu and Cm, are crucial [84]. Efficiently tracking actinide levels also minimizes losses to waste streams, and enhancing the overall process efficiency by optimizing electrorefining and electrowinning process by combining with computational models. In electrorefining stages, the concentration of U typically starts high (~ 10 wt%) [86] and decreases as it is deposited, whereas Pu concentration increases as it is dissolved from SNF. During electrowinning, the process duration and termination are dictated by the targeted actinide concentrations.

Fission products, including lanthanides (La, Ce, Nd, Sm, etc.), Cs, Sr, Zr, and noble metals, are diverse and abundant in pyroprocessing [9]. Monitoring these elements is essential for several reasons: evaluating the separation efficiency of electrorefining, controlling impurities that may impact process or product quality [9], and managing waste streams for safe disposal. The presence and buildup of specific fission products can significantly affect the efficiency [87] and safety of the process.

Oxygen concentration plays a critical role in the oxide reduction process in pyroprocessing [25, 39, 41]. Proper

Table 3 Major target elements for monitoring in pyroprocessing

Major element	Pyroprocessing stage	Necessity for measurement	Electrochemical measurement feasibility	Electrochemical property measurement references	Remarks
U	Electrorefining, electrowinning	Process efficiency (purity of the product, signal of moving to next step), nonproliferation	Yes	[29, 30, 110, 131–136]	High concentration measurements method is needed
Pu	Electrorefining, electrowinning	Process efficiency (purity of the product, signal of moving to next step), nonproliferation	Yes	[29, 131, 132, 137]	Multi-element measurement method is needed
Cm	Electrorefining, electrowinning	Nonproliferation	Yes	[138, 139]	Multi-element measurement method is needed
Zr	Electrorefining, electrowinning	Process efficiency (purity of the product)	Yes	[140–146]	–
Sr	Oxide reduction	Waste management (highly heat generating elements—high level waste (waste volume))	No	–	–
Rare earth elements	Electrorefining, electrowinning	Process efficiency (TRU ingot quality, TRU ingot proliferation)	Yes	La [147–150], Ce[151, 152], Nd [132, 153], Sm[154, 107, 108]	Multi-element measurement method is needed
Oxygen	Oxide reduction	Process efficiency	Yes	[92, 94]	–

management of oxygen levels is also crucial for protecting anode material which is precious metallic Pt [34]. During oxide reduction processes, the method of oxygen removal varies: in electrolytic reduction, oxygen is extracted at the anode, while in chemical reduction, it reacts to form Li_2O. A 2–3 wt% of Li_2O is considered as ideal for the oxide reduction process [4]. Throughout pyroprocessing, maintaining precise control over oxygen concentrations is vital to prevent the unwanted precipitation of oxides [58].

Electrochemical Sensor for Pyroprocessing Monitoring

Electrochemical sensors, crucial for analyzing molten salt compositions and monitoring corrosion within pyroprocessing, are under development. These sensors, classified into voltammetric and amperometric types, offer real-time measurement capabilities across the extensive electrochemical window of molten salts, maintaining functionality even under high radiation levels [28–30, 35]. However, operating at high temperatures (650 °C for oxide reduction and 500 °C for electrorefining and electrowinning) presents significant challenges for long-term stability and reliability of electrochemical sensors. High-temperature environments can cause material degradation and corrosion, significantly limiting the choice of durable materials for sensor components. For example, Pyrex is a useful ceramic material for reference electrodes; however, it is unsuitable above 600 °C due to phase transitions that cause structural failures [88]. Especially, defining the surface area of the working electrode is challenging due to the fluctuation in salt levels during the process [28–30]. Fluctuation in salt levels can cause thermal fatigue of sensor material by cyclical changes in temperature. Furthermore, pyroprocessing operates in a salt that dissolve diverse elements, from relatively high concentrations of U to lower concentrations of actinides such as Am, Np, and lanthanides such as Nd and La. It is challenging to measure ion concentration using electrochemical techniques when multiple other ions are present in higher concentrations [37, 89–91]. Deploying these sensors in flow environments introduces additional challenges, including the significant impact of natural convection on electrochemical measurements.

Current State-of-the-Art: Materials

One of the critical challenges in the implementation of pyroprocessing is the material degradation and corrosion

that occur in high-temperature molten salt environments. This degradation primarily affects the longevity and reliability of sensor components crucial for monitoring and controlling the electrochemical processes. High temperatures combined with corrosive molten salts can lead to accelerated wear and tear on conventional materials (such as Teflon, plastic) used in manufacturing sensors. For molten salt monitoring electrode materials, both metal and carbon (e.g., glassy carbon, graphite) are utilized. W [92], Mo [93], Ta [94], and Pt [57] are preferred for working and counter electrodes due to their stability in chloride and fluoride molten salt environments [95]. Ceramic materials like alumina, boron nitride (BN), magnesium oxide (MgO), quartz, and Pyrex serve various roles, including in sensor bodies and membranes, chosen for their durability at high temperatures [88, 96–100].

The material of the working electrode determines the electrochemical potential window. Cyclic voltammograms obtained from Mo, Pt, W, and C electrodes in LiCl molten salt are shown in Fig. 8. The cathodic limit of Pt and C occurs at higher voltages due to lithium deposition than Mo and W. Cathodic limit decided by the deposition potential of intermetallic compound of metal and major cation such as Li^+ and K^+ or Li metal. The anodic limit occurs in the order of Mo, W, and Pt by the anodic dissolution of metal, while chlorine gas evolution reactions set the anodic limit at carbon electrodes. Therefore, the selection of working electrode materials should consider the electrochemical window depending on the element of interest.

Reference electrodes, vital for precise potential measurements, vary based on the salt composition and operational temperature. In oxide reduction processes using LiCl-Li_2O [57, 101, 102], Bi-Li alloys [102], Ni/NiO [39, 52, 55, 92, 103, 104], and quasi-reference electrodes such as Pt [52] are utilized. For electrorefining processes in LiCl–KCl, Ag/AgCl [92, 105] electrodes are commonly used. The membrane material for these reference electrodes in high-temperature applications includes Pyrex, alumina, mullite ($3Al_2O_3{\cdot}2SiO_2$), and quartz, selected for their high-temperature resilience [88]. For instance, mullite, while excellent for high-temperature applications above 650 °C due to its stability and low potential deviations, is less suitable for the lower temperatures typical of electrorefining and electrowinning processes. Additionally, the considerable time mullite requires to reach equilibrium can hinder efficiency in processes that necessitate quick sensor responses. Pyrex faces its own set of challenges, particularly its vulnerability to phase transitions around 600 °C [106]. This characteristic makes it less ideal for processes like oxide reduction, which operates around 650 °C. The structural changes induced by exposure to high temperatures can cause deformations or failures in the sensor, compromising measurement integrity and accuracy. Quartz, although it demonstrates good mechanical strength and stability at temperatures exceeding 800 °C, is not as effective in the temperature range of 500 °C to 650 °C, which is crucial for many nuclear recycling processes. The lengthy stabilization period needed for quartz at these temperatures can impact the speed and

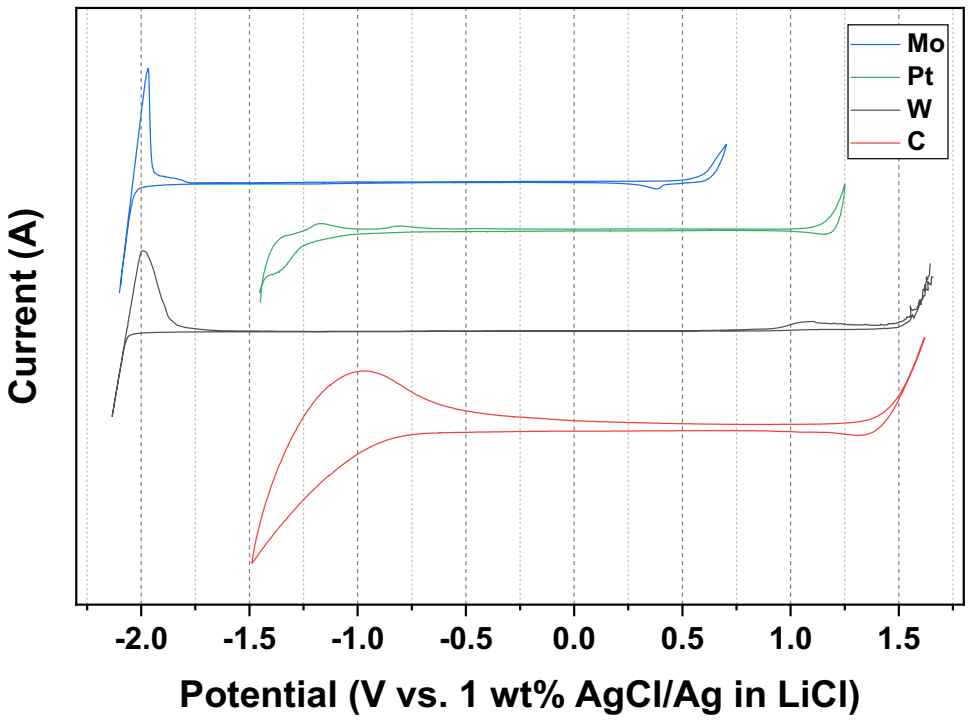

Fig. 8 Cyclic voltammograms obtained from Mo, Pt, W, and C electrode in 923 K LiCl molten salt

efficiency of electrochemical reactions, posing a problem for precise process control and throughput. These examples underscore the importance of selecting the appropriate membrane based on the specific operational requirements and the challenges of high-temperature conditions in pyroprocessing environments.

Challenge and Solving Approach: Surface Area of Working Electrode

Voltammetry, a technique that measures changes in current in response to voltage alterations, relies on the proportionality between the current magnitude and the working electrode's surface area. Accurately determining this surface area is crucial for precise measurements but poses challenges in molten salt environments due to the high temperatures and reactive nature of the salts against structural materials for electrodes. One way to define the surface area is by using metal electrodes encased in non-conductive materials such as glass or ceramic [30, 107, 108]. However, this approach is limited by the potential reaction between the non-conductive material and the molten salt, and the differential thermal expansion between materials, which can lead to cracking. In the case of W, it was confirmed that the thermal expansion coefficient has a range of $4.358 \sim 5.160 \times 10^{-6}$ $℃^{-1}$ from room temperature to 1000 ℃ through the relationship with temperature [109]. In the case of alumina, the thermal expansion coefficient was confirmed to have a value of $7 \sim 9 \times 10^{-6}$ $℃^{-1}$. The difference in thermal expansion values between alumina and W can cause stress and cracking in the alumina. Therefore, if the method of encapsulating with nonconductive material is chosen, the nonconductive material should be selected to minimize the difference in thermal expansion with metal electrodes.

Another approach to accurately define the surface area of the working electrode involves utilizing a vertical translator to precisely adjust the electrode's exposure [29, 110]. Tylka et al. developed a method, that improves upon traditional techniques, using surface area difference and cathodic peak current difference measured by changing the depth of the electrode using a vertical translator, significantly enhancing measurement accuracy [29]. This method allows for actinide (U, Pu) measurement with cyclic voltammetry (CV) technique and the concentration measured with electroanalytical method show good agreement with the concentration measured by ICP-AES. However, this approach may be dependent on the U concentration in the salt. In high concentration environments, the signal in the cyclic voltammogram can become saturated, potentially hindering accurate measurements. Similarly, Rappleye et al. used the same technique to control of the surface area and tested various electrochemical techniques (CV, NPV, CA, and OCP) to measure U and Mg binary mixture [110]. Their work showed that NPV was found to be the most accurate method for measuring the concentrations for U and Mg in molten salts. Together, these studies present the method to solve surface area problem by using vertical translator and CV measurements. However, the measurement for correcting the electrode area should be conducted at least twice, and measurement at another time causes an error because it is impossible to distinguish between the concentration change and the electrode area change.

The other approach is that the surface area of electrodes can be calculated by using the current peak difference between electrodes with known length differences [28]. The method using a reduction peak current to define the surface area immersed in molten salt has an advantage for long-term in-situ monitoring. This method has the advantage of long-term stability because of its simple working electrode configuration which are metal rods. However, this method using the Randles–Sevcik equation operates under several assumptions: there is no mass transport by migration or convection; the reaction is reversible and diffusion-limited; the activity of the deposited substance is assumed to be unity; and the diffusion process is approximated as linear [111]. The use of this method for process monitoring is limited by these assumptions, especially since forced or natural convection is difficult to avoid in pyroprocessing [108, 112]. To handle the problem, machine learning can be the solution [113]. The surface area predicting model could be trained with electrochemical data with multiarray electrodes from the simulated pyroprocessing environment.

Challenge and Solving Approach: Multi-element Environment

The interpretation of cyclic voltammograms transcends the simplistic linear superposition of individual responses due to the manifestation of electrochemical–chemical–electrochemical (ECE) reaction mechanisms in a multi-species environment. This complexity underscores the inadequacy of directly summing the voltammetric responses, as it overlooks the nuanced interdependencies introduced by intervening chemical reactions.

In such environments where multi-element ions coexist, both oxidation–reduction reactions between ions and deposited metal coexist. This results in the simultaneous presence of electrochemical and chemical reactions. Consequently, the cyclic voltammogram is different from the simplistic linear superposition of individual cyclic voltammograms due to chemical reaction with deposited metal and the other metal ions in molten salt (ECE reaction) (Fig. 9) [111, 114]. In addition, metal deposition on the working electrode while performing the electrochemical measurement causes an increase in the working electrode's surface area. The change in the surface area of the working electrode

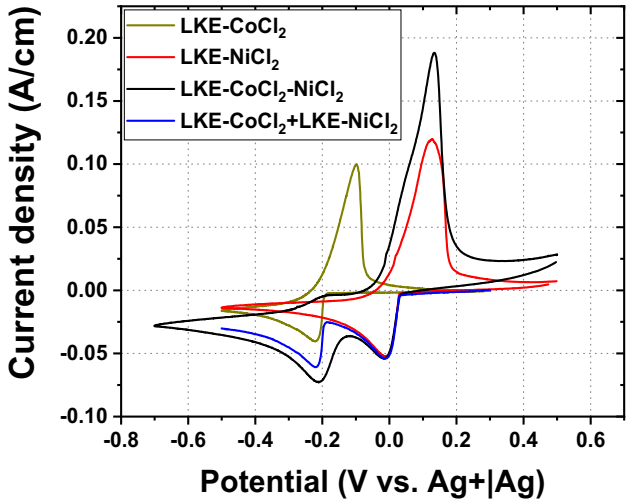

Fig. 9 Changes in cyclic voltammogram (CV) in a multi-element environment (LiCl–KCl eutectic (LKE)–$CoCl_2$–$NiCl_2$) from Sum of CV of LKE-$CoCl_2$ and CV of LKE–$NiCl_2$ (LKE–$CoCl_2$ + LKE–$NiCl_2$) due to electrochemical-chemical-electrochemical (ECE) reactions [114]

by deposited metal on electrode while measuring causes a non-linear relationship between concentration and current.

Researchers have explored various electrochemical detection methods to address the challenges of correlating concentration with current in multi-element environments. Lizuka et al. used normal pulse voltammetry (NPV) and square wave voltammetry (SWV) for measuring U, Pu, Gd, and Np in a coexisting salt matrix [91]. NPV showed a robust approach for the actinide concentration measurement method, in the presence of Gd, without interference from other components. Huan Zhang et al. investigated the use of CV and SWV for real-time measurement of minor metal ion concentration (using $CeCl_3$ as a surrogate for $PuCl_3$) in the presence of high concentrations of UCl_3 [37]. They were able to obtain reproducible peak currents for $CeCl_3$, and as the concentration of U increased from 5 wt% to 10 wt%, the peak current for $CeCl_3$ increased by only 8.3%. pulse voltammetry such as NPV and SWV show potential for a multi-element environment, however, as an in-situ monitoring method it appears to be inappropriate. This is because, pulse voltammetry requires fine voltage control, but in high-radiation environments, measurements necessitate longer cables for equipment shielding from radiation, which acts as noise [115] and imposes limitations on real-time measurements due to the difficulty in fine voltage control. Secondly, compared to CV, the longer measurement times of SWV imply a longer response time. If the response time is too long, valuable information in the process data may be lost, and fault information cannot be obtained promptly [116].

In an aqueous system, strategies to overcome the difficulty of multi-element detection are developed using microfluidic devices or microelectrodes [117–119], but these methods cannot be used in high-temperature molten salts because of the absence of long-term stability of microelectrodes and absence of microfluidic devices used at process temperatures [108, 120, 121]. Recently, the method of combining AI algorithms and electrochemical measurements has been widely investigated, but it requires big data for training the AI algorithm [122, 123]. By employing parallel electrochemical cells to gather measurement data across varied concentration environments, it is feasible to collect a dataset adequate for training AI algorithms, potentially overcoming the multi-element detection challenge.

Challenge and Solving Approach: Flow environment

Electrochemical sensors developed in the static environment for molten salt applications may face significant challenges when deployed in flow environments [70]. Recent research underscores the profound influence of natural convection on electrochemical measurements [112, 124]. Notably, Ge et al. showed abnormal natural convection patterns observed in molten LiCl–KCl, showing its arising time varied with temperature, significantly influencing electrochemical measurements [112]. Although the use of microelectrodes has been proposed to mitigate these effects, their long-term stability in molten salt conditions remains unproven [108]. In addition, Zhu et al. detailed an in situ method to measure the concentration of soluble redox species in molten LiCl–KCl by combining simulation natural convection environment [124]. Their study verified the presence of strong natural convection leading to steady-state currents during CV tests at low scan rates, suggesting a novel methodology to assess diffusion coefficients and concentration ratios by utilizing natural convection phenomena.

Simulating molten salt flow presents a viable strategy for improving the accuracy and reliability of electrochemical analysis in dynamic environments. This approach could lead to the development of new empirical models that more accurately describe ion concentrations in fluctuating molten salt systems. A suggestion by Zhe et al. involves the introduction of a concentration correction factor that could effectively integrate flow considerations into analytical frameworks. In addition, by collecting simulated electrochemical data with various geometry of electrode from simulated flow environments and applying machine learning techniques, it is possible to optimize various electrode designs could have a simple concentration correction factor or a simulated empirical model [125].

Conclusion

This review has systematically explored the molten salt processes involved in pyroprocessing, the critical role of monitoring, the significance of major elements, and the current

developments, challenges, and future directions for electrochemical sensors in the pyroprocessing of SNF. Integrating AI with electrochemical techniques emerges as a promising approach to existing challenges, such as accurately determining the working electrode's surface area and achieving selective measurements in environments with multiple elements. The other future research direction is development of advanced electrode including long-term stability microelectrodes and flow optimized electrode. The integration of flow condition computational models and experimental data in static cells through machine learning algorithms can give flow optimized electrode that optimized to give have a simple concentration correction factor or a simulated empirical model. Such advancements in electrochemical sensor technology mark significant progress toward the realization of sustainable nuclear energy, enhancing economic, safety, and nonproliferation aspects of process monitoring.

Acknowledgements This work was financially supported by National Research Foundation of Korea (NRF) grant funded by the Ministry of Science and ICT, Republic of Korea, (NRF-2022M2D4A1052797, NRF-2020M2D4A1070724) and was supported by the Korea Institute of Energy Technology Evaluation and Planning (KETEP) and the Ministry of Trade, Industry & Energy (MOTIE) of the Republic of Korea (No. 20224000000120).

Data availability The datasets used and/or analyzed during the current study are available from the corresponding author upon reasonable request.

References

1. A.V. Soler, The future of nuclear energy and small modular reactors, in *Living with climate change*. (Elsevier Inc., Amsterdam, 2024). https://doi.org/10.1016/B978-0-443-18515-1.00012-5
2. P.A. DeCotis, E.D. Cartwright, The role of small modular reactors in decarbonization. Clim. Energy **38**, 12–17 (2022). https://doi.org/10.1002/gas.22290
3. C.A. Coffey, Small modular reactor technology for industrial heat and power : selection techniques and implementation strategies for real-world use cases using systems-based approaches. by, Massachusetts Institute of Technology. 2023
4. International Atomic Energy Agency, Status and trends in pyroprocessing of spent nuclear fuels, IAEA-TECDOC-1967. (IAEA, Vienna, 2021)
5. M.-S. Yim, *Nuclear waste management* (Springer Netherlands, Dordrecht, 2022). https://doi.org/10.1007/978-94-024-2106-4
6. C. Corkhill, N. Hyatt, *Nuclear waste management* (IOP Publishing, Bristol, 2018)
7. N. Chae, S. Park, S. Seo, R.I. Foster, H. Ju, S. Choi, Coupled mixed-potential and thermal-hydraulics model for long-term corrosion of copper canisters in deep geological repository. Npj Mater. Degrad. **7**, 1–14 (2023). https://doi.org/10.1038/s41529-023-00345-6
8. G.L. Fredrickson, T. Yoo, Engineering scale pyroprocessing activities in the United States, TLR-RES/DE/REB-2023-10, Idaho Natl. Lab. (2023). https://www.nrc.gov/docs/ML2335/ML23353A049.pdf
9. H.-S.H. Lee, G.-I. Park, K.-H. Kang, J.-M. Hur, J.-G. Kim, D.-H. Ahn, Y.-Z. Cho, E.-H. Kim, Pyroprocessing technology development at KAERI. Nucl. Eng. Technol. **43**, 317–328 (2011). https://doi.org/10.5516/NET.2011.43.4.317
10. M.F. Simpson, Developments of spent nuclear fuel pyroprocessing technology at Idaho national laboratory, INL/EXT-12-25124. Idaho Natl. Lab., 1–21 (2012). https://doi.org/10.2172/1044209
11. T. Inoue, T. Koyama, Y. Arai, State of the art of pyroprocessing technology in Japan. Energy Procedia. **7**, 405–413 (2011). https://doi.org/10.1016/j.egypro.2011.06.053
12. M.A. Rose, W.C. Phillips, R.O. Hoover, M.E. Woods, An assessment of applying pyroprocessing technology to advanced pebble-type fuels, ANL/CFCT-23/6 Rev. 1. Argonne Natl. Lab., (2023). https://publications.anl.gov/anlpubs/2023/09/184675.pdf
13. J.B. Coble, S.E. Skutnik, S.N. Gilliam, M.P. Cooper, Review of candidate techniques for material accountancy measurements in electrochemical separations facilities. Nucl. Technol. **206**, 1803–1826 (2020). https://doi.org/10.1080/00295450.2020.1724728
14. D.R. Olander, Nucleauclear fuels present and future. Eng. J. **13**, 1–28 (2009). https://doi.org/10.4186/ej.2009.13.1.1
15. S.M. Woo, S.S. Chirayath, M. Fuhrmann, Nuclear fuel reprocessing: can pyro-processing reduce nuclear proliferation risk? Energy Polic. (2020). https://doi.org/10.1016/j.enpol.2020.111601
16. R. Taylor, G. Mathers, A. Banford, The development of future options for aqueous recycling of spent nuclear fuels. Prog. Nucl. Energy **164**, 104837 (2023). https://doi.org/10.1016/j.pnucene.2023.104837
17. R.I. Foster, J.K. Park, K. Lee, B.-K. Seo, UK civil nuclear decommissioning, a blueprint for Korea's nuclear decommissioning future?: part I-nuclear legacy, strategies, and the NDA. J. Nucl. Fuel Cycle Waste Technol. **19**, 387–419 (2021). https://doi.org/10.7733/jnfcwt.2021.19.3.387
18. R.I. Foster, J.K. Park, K. Lee, B.-K. Seo, UK civil nuclear decommissioning, a blueprint for Korea's nuclear decommissioning future?: part II–UK's progress and implications for Korea. J. Nucl. Fuel Cycle Waste Technol. **20**, 65–98 (2022). https://doi.org/10.7733/jnfcwt.2022.006
19. T. Grebennikova, A.N. Jones, C.A. Sharrad, Electrochemical decontamination of irradiated nuclear graphite from corrosion and fission products using molten salt. Energy Environ. Sci. **14**, 5501–5512 (2021). https://doi.org/10.1039/D1EE00332A
20. M.L. Remerowski, 238Pu recovery and salt disposition from the molten salt oxidation process, In: AIP Conf. Proc., AIP, pp. 246–247 (2000). https://doi.org/10.1063/1.1292280
21. D.Q. Gbadago, J. Moon, S. Hwang, Exploring advanced process equipment visualization as a step towards digital twins development in the chemical industry: a CFD-DNN approach. Korean J. Chem. Eng. **40**, 37–45 (2023). https://doi.org/10.1007/s11814-022-1273-2
22. H.M.A. Shahzad, S.J. Khan, M. Khan, H. Schönberger, F.A. Weber, Performance and cost-benefit analysis of anaerobic moving bed biofilm reactor for pretreatment of textile wastewater. Korean J. Chem. Eng. **40**, 1389–1400 (2023). https://doi.org/10.1007/s11814-022-1334-6
23. Y. Zhou, Z. Cao, J. Lu, C. Zhao, D. Li, F. Gao, Objectives, challenges, and prospects of batch processes: arising from injection molding applications. Korean J. Chem. Eng. **39**, 3179–3189 (2022). https://doi.org/10.1007/s11814-022-1294-x
24. A.N. Williams, G. Cao, M.R. Shaltry, Voltammetry measurements in lithium chloride-lithium oxide (LiCl–Li_2O) salt: an evaluation of working electrode materials. J. Nucl. Mater. (2021). https://doi.org/10.1016/j.jnucmat.2020.152760
25. S.H. Park, S.K. Han, S.K. Ahn, Monitoring of oxygen in simulated electrolytic reduction salt of pyroprocessing using laser-induced breakdown spectroscopy. Appl. Spectrosc. **75**, 1358–1363 (2021). https://doi.org/10.1177/00037028211042873

26. M.C. Miller, G. Cao, G. Galbreth, S.X. Li, M. Shaltry, J.D. Sanders, B. Westphal, A.N. Williams, Pyroprocessing monitoring technology development at Idaho national laboratory, In: Proc. Glob. 2017 (Seoul, Korea KRS, 2017), 2017
27. E.Y. Choi, S.M. Jeong, Electrochemical processing of spent nuclear fuels: an overview of oxide reduction in pyroprocessing technology. Prog. Nat. Sci. Mater. Int. **25**, 572–582 (2015). https://doi.org/10.1016/j.pnsc.2015.11.001
28. J. Guo, N. Hoyt, M. Williamson, Multielectrode array sensors to enable long-duration corrosion monitoring and control of concentrating solar power systems. J. Electroanal. Chem. **884**, 115064 (2021). https://doi.org/10.1016/j.jelechem.2021.115064
29. M.M. Tylka, J.L. Willit, J. Prakash, M.A. Williamson, Method development for quantitative analysis of actinides in molten salts. J. Electrochem. Soc. **162**, H625–H633 (2015). https://doi.org/10.1149/2.0401509jes
30. D. Rappleye, K. Teaford, M.F. Simpson, Investigation of the effects of uranium(III)-chloride concentration on voltammetry in molten LiCl–KCl eutectic with a glass sealed tungsten electrode. Electrochim. Acta **219**, 721–733 (2016). https://doi.org/10.1016/j.electacta.2016.10.075
31. D.H. Kim, S.E. Bae, T.H. Park, J.Y. Kim, C.W. Lee, K. Song, Real-time monitoring of metal ion concentration in LiCl–KCl melt using electrochemical techniques. Microchem. J. **114**, 261–265 (2014). https://doi.org/10.1016/j.microc.2014.01.011
32. C. Zhang, D. Rappleye, A. Nelson, S. Simpson, M. Simpson, Electroanalytical measurements of oxide ions in molten $CaCl_2$ on W electrode. J. Electrochem. Soc. **168**, 097502 (2021). https://doi.org/10.1149/1945-7111/ac208e
33. K.S. Mohandas, Direct electrochemical conversion of metal oxides to metal by molten salt electrolysis: a review. Trans. Inst. Min Metall. Sect. C Miner. Process. Extr. Metall. **122**, 195–212 (2013). https://doi.org/10.1179/0371955313Z.00000000069
34. S.M. Jeong, H.S. Shin, S.H. Cho, J.M. Hur, H.S. Lee, Electrochemical behavior of a platinum anode for reduction of uranium oxide in a LiCl molten salt. Electrochim. Acta **54**, 6335–6340 (2009). https://doi.org/10.1016/j.electacta.2009.05.080
35. G. Mamantov, D.L. Manning, Voltammetry and related studies of uranium in molten lithium fluoride-beryllium fluoride-zirconium fluoride. Anal. Chem. **38**, 1494–1498 (1966). https://doi.org/10.1021/ac60243a010
36. M.M. Tylka, J.L. Willit, J. Prakash, M.A. Williamson, Application of voltammetry for quantitative analysis of actinides in molten salts. J. Electrochem. Soc. **162**, H852–H859 (2015). https://doi.org/10.1149/2.0281512jes
37. H. Zhang, S. Choi, C. Zhang, E. Faulkner, N. Alnajjar, P. Okabe, D.C. Horvath, M.F. Simpson, Square wave voltammetry for real time analysis of minor metal ion concentrations in molten salt reactor fuel. J. Nucl. Mater. **527**, 151791 (2019). https://doi.org/10.1016/j.jnucmat.2019.151791
38. C.Y. Jung, T.H. Kim, S.E. Bae, Real-time monitoring of uranium concentration in NaCl–$MgCl_2$–UCl_3 molten salt. J. Radioanal. Nucl. Chem. **332**, 5233–5238 (2023). https://doi.org/10.1007/s10967-023-09000-5
39. A.I. Valtseva, P.S. Pershin, A.S. Kalyakin, A.N. Volkov, A. V. Suzdaltsev, Y.P. Zaikov, Development of oxygen sensor for pyrochemical reactors of spent nuclear fuel reprocessing, In: J. Phys. Conf. Ser., institute of physics publishing. (2020). https://doi.org/10.1088/1742-6596/1565/1/012050
40. H. Zheng, H. Nian, J. Xia, G. Zhou, D. Jiang, Q. Li, Bi/Bi2O3 sensor for quantitation of dissolved oxygen in molten salts. J. Adv. Ceram. **7**, 1–4 (2018). https://doi.org/10.1007/s40145-017-0250-4
41. F. Felling, O.R. Dale, M. Gonzalez, C. Zhang, M.F. Simpson, Application of cyclic voltammetry with W electrodes for measurement of high CaO concentration in molten $CaCl_2$. J. Electrochem. Soc. **171**, 017514 (2024). https://doi.org/10.1149/1945-7111/ad1eca
42. E.Y. Choi, I.K. Choi, J.M. Hur, D.S. Kang, H.S. Shin, S.M. Jeong, In situ electrochemical measurement of O_2- concentration in molten Li_2OLiCl during uranium oxide reduction process. Electrochem. Solid State Lett. **15**, 11–14 (2012). https://doi.org/10.1149/2.016203esl
43. D.K. Corrigan, J.P. Elliott, E.O. Blair, S.J. Reeves, I. Schmüser, A.J. Walton, A.R. Mount, Advances in electroanalysis, sensing and monitoring in molten salts. Faraday Discuss. **190**, 351–366 (2016). https://doi.org/10.1039/C6FD00002A
44. W. Yang, Machine learning-based electrochemical monitoring for molten chloride salt reactors, Ph. D. thesis, Korea advanced institute of science and technology, Daejeon (2024).
45. W. Yang, Y. Choi, S. Choi, S. Choi, Development of machine learning model for estimating electrode surface area via cyclic voltammetry using two rod electrodes in molten salts, In: 16th Inf. Exch. Meet. Actin. Fission Prod. Partitioning transmutat. (2023)
46. J. Bruno, L. Duro, F. Diaz-Maurin, Spent nuclear fuel and disposal, in *Advances in nuclear fuel chemistry*. (Woodhead Publishing, Cambridge, 2020), pp. 527–553. https://doi.org/10.1016/B978-0-08-102571-0.00014-8
47. J. Bruno, R.C. Ewing, Spent nuclear fuel. Elements **2**, 343–349 (2006). https://doi.org/10.2113/gselements.2.6.343
48. E.-Y. Choi, J.-K. Kim, H.-S. Im, I.-K. Choi, S.-H. Na, J.W. Lee, S.M. Jeong, J.-M. Hur, Effect of the UO_2 form on the electrochemical reduction rate in a LiCl–Li_2O molten salt. J. Nucl. Mater. **437**, 178–187 (2013). https://doi.org/10.1016/j.jnucmat.2013.01.306
49. J.M. Shin, J.J. Park, J.W. Lee, J.W. Lee, Optimization of off-gas trapping capabilities on pyroprocessing at KAERI (2009), https://inis.iaea.org/search/search.aspx?orig_q=RN:41070517. Accessed 25 Mar 2024
50. G. Il Park, M.K. Jeon, J.H. Choi, K.R. Lee, S.Y. Han, I.T. Kim, Y.Z. Cho, H.S. Park, Recent progress in waste treatment technology for pyroprocessing at KAERI. J. Nucl. Fuel Cycle Waste Technol. **17**, 279–298 (2019). https://doi.org/10.7733/jnfcwt.2019.17.3.279
51. W. Park, J.K. Kim, J.M. Hur, E.Y. Choi, H.S. Im, S.S. Hong, Application of a boron doped diamond (BDD) electrode as an anode for the electrolytic reduction of UO_2 in Li_2O–LiCl–KCl molten salt. J. Nucl. Mater. **432**, 175–181 (2013). https://doi.org/10.1016/j.jnucmat.2012.08.005
52. T.B. Joseph, N. Sanil, K.S. Mohandas, K. Nagarajan, A study of graphite as anode in the electro-deoxidation of solid UO_2 in LiCl–Li_2O melt. J. Electrochem. Soc. **162**, E51–E58 (2015). https://doi.org/10.1149/2.0521506jes
53. Y. Sakamura, Effect of alkali and alkaline-earth chloride addition on electrolytic reduction of UO_2 in LiCl salt bath. J. Nucl. Mater. **412**, 177–183 (2011). https://doi.org/10.1016/j.jnucmat.2011.02.055
54. D. Kang, N. Chae, W. Yang, S. Yoon, R.I. Foster, J.T.M. Amphlett, S.E. Bae, E.Y. Choi, S. Choi, Investigation of dissolution behavior of SrO in molten LiCl–KCl salts for heat reduction of used nuclear fuel. J. Nucl. Mater. **562**, 153615 (2022). https://doi.org/10.1016/j.jnucmat.2022.153615
55. S.D. Herrmann, S.X. Li, Separation and recovery of uranium metal from spent light water reactor fuel via electrolytic reduction and electrorefining. Nucl. Technol. **171**, 247–265 (2010). https://doi.org/10.13182/NT171-247
56. W. Park, E.Y. Choi, S.W. Kim, S.C. Jeon, Y.H. Cho, J.M. Hur, Electrolytic reduction of a simulated oxide spent fuel and the fates of representative elements in a Li_2O–LiCl molten salt. J. Nucl. Mater. **477**, 59–66 (2016). https://doi.org/10.1016/j.jnucmat.2016.04.058

57. E.Y. Choi, C.Y. Won, J.S. Cha, W. Park, H.S. Im, S.S. Hong, J.M. Hur, Electrochemical reduction of UO_2 in LiCl–Li_2O molten salt using porous and nonporous anode shrouds. J. Nucl. Mater. **444**, 261–269 (2014). https://doi.org/10.1016/j.jnucmat.2013.09.061
58. B.H. Park, S.B. Park, S.M. Jeong, C.S. Seo, S.W. Park, Electrolytic reduction of spent oxide fuel in a molten LiCl–Li_2O system. J. Radioanal. Nucl. Chem. **270**, 575–583 (2006). https://doi.org/10.1007/s10967-006-0464-3
59. J.J. Laidler, J.E. Battles, W.E. Miller, J.P. Ackerman, E.L. Carls, Development of pyroprocessing technology. Prog. Nucl. Energy **31**, 131–140 (1997). https://doi.org/10.1016/0149-1970(96)00007-8
60. K.R. Kim, S.Y. Choi, D.H. Ahn, S. Paek, B.G. Park, H.S. Lee, K.W. Yi, I.S. Hwang, Computational analysis of a molten-salt electrochemical system for nuclear waste treatment. J. Radioanal. Nucl. Chem. **282**, 449–453 (2009). https://doi.org/10.1007/s10967-009-0171-y
61. S. Choi, J. Park, R.O. Hoover, S. Phongikaroon, M.F. Simpson, K.R. Kim, I.S. Hwang, Uncertainty studies of real anode surface area in computational analysis for molten salt electrorefining. J. Nucl. Mater. **416**, 318–326 (2011). https://doi.org/10.1016/j.jnucmat.2011.06.020
62. S. Seo, S. Choi, B.G. Park, Transient modeling of spent nuclear fuel electrorefining with liquid metal electrode. J. Nucl. Mater. **491**, 115–125 (2017). https://doi.org/10.1016/j.jnucmat.2017.04.053
63. M. Brigaudeau, P. Chardard, Study of electrochemical properties of uranium in a molten fluoride medium (1979), https://inis.iaea.org/search/search.aspx?orig_q=RN:11534799. Accessed 25 Mar 2024
64. M.R. Hale, Argonne national laboratory 1985 publications, Argonne, IL. (1987). https://doi.org/10.2172/6197639
65. S.L. Marshall, L. Redey, G.F. Vandegrift, D.R. Vissers, Electroformation of uranium hemispherical shells, ANL-89/26, Argonne, IL (United States). (1989). https://doi.org/10.2172/5274651
66. Y.H. Kang, J.H. Lee, S.C. Hwang, J.B. Shim, E.H. Kim, S.W. Park, Electrodeposition characteristics of uranium by using a graphite cathode. Carbon **44**, 3142–3145 (2006). https://doi.org/10.1016/j.carbon.2006.05.026
67. C.H. Lee, T.J. Kim, S. Park, S.J. Lee, S.W. Paek, D.H. Ahn, S.K. Cho, Effect of cathode material on the electrorefining of U in LiCl–KCl molten salts. J. Nucl. Mater. **488**, 210–214 (2017). https://doi.org/10.1016/j.jnucmat.2017.03.023
68. Y.H. Kang, S.C. Hwang, H.S. Lee, E.H. Kim, S.W. Park, J.H. Lee, Effects of neodymium oxide on an electrorefining process of uranium. J. Mater. Process. Technol. **209**, 5008–5013 (2009). https://doi.org/10.1016/j.jmatprotec.2009.01.024
69. T. Koyama, M. Iizuka, Y. Shoji, R. Fujita, H. Tanaka, T. Kobayashiz, M. Tokiwai, An experimental study of molten salt electrorefining of uranium using solid iron cathode and liquid cadmium cathode for development of pyrometallurgical reprocessing. J. Nucl. Sci. Technol. **34**, 384–393 (1997). https://doi.org/10.1080/18811248.1997.9733678
70. S. Choi, J. Park, K.R. Kim, H. Jung, I. Hwang, B. Park, K. Yi, H.S. Lee, D. Ahn, S. Paek, Three-dimensional multispecies current density simulation of molten-salt electrorefining. J. Alloys Compd. **503**, 177–185 (2010). https://doi.org/10.1016/j.jallcom.2010.04.228
71. T. Koyama, M. Lizuka, N. Kondo, R. Fujita, H. Tanaka, Electrodeposition of uranium in stirred liquid cadmium cathode. J. Nucl. Mater. **247**, 227–231 (1997). https://doi.org/10.1016/S0022-3115(97)00100-1
72. D. Ahn, S. Paek, J. Shim, K. Kim, T. Kim, J. Jung, G. Kim, Development of the electrowinning technology for TRU recovery in pyroprocessing, In: 2012 Trans. Korean Nucl. Soc. Spring Meet., Korean Nuclear Society. (2012)
73. K. Liu, L.Y. Yuan, Y.L. Liu, X.L. Zhao, H. He, G.A. Ye, Z.F. Chai, W.Q. Shi, Electrochemical reactions of the Th^{4+}/Th couple on the tungsten, aluminum and bismuth electrodes in chloride molten salt. Electrochim. Acta **130**, 650–659 (2014). https://doi.org/10.1016/j.electacta.2014.03.085
74. Y. Sakamura, O. Shirai, T. Iwai, Y. Suzuki, Thermodynamics of neptunium in LiCl–KCl eutectic/liquid bismuth systems. J. Electrochem. Soc. **147**, 642 (2000). https://doi.org/10.1149/1.1393246
75. T. Yin, Y. Liu, D. Yang, Y. Yan, G. Wang, Z. Chai, W. Shi, Thermodynamics and kinetics properties of lanthanides (La, Ce, Pr, Nd) on liquid bismuth electrode in LiCl–KCl molten salt. J. Electrochem. Soc. **167**, 122507 (2020). https://doi.org/10.1149/1945-7111/abb0f4
76. K. Kinoshita, T. Inoue, S.P. Fusselman, D.L. Grimmett, J.J. Roy, R.L. Gay, C.L. Krueger, C.R. Nabelek, T.S. Storvick, Separation of uranium and transuranic elements from rare earth elements by means of multistage extraction in LiCl–KCl/Bi system. J. Nucl. Sci. Technol. **36**, 189–197 (1999). https://doi.org/10.1080/18811248.1999.9726197
77. S. Sohn, G.Y. Jeong, S. Jeong, J. Hur, H. Ju, Y.H. Shin, J. Park, I.S. Hwang, Spatial distribution of $CeBi_2$ in Bi–Ce alloy facilitating density-based separation between actinides and lanthanides. J. Nucl. Mater. **526**, 151750 (2019). https://doi.org/10.1016/j.jnucmat.2019.151750
78. S. Paek, S.-H. Kim, D. Yoon, T.-J. Kim, D.-H. Ahn, H. Lee, Electrochemical study on various types of anode materials in LiCl–KCl eutectic salt used in the electro-winning process. J. Radioanal. Nucl. Chem. **295**, 439–444 (2013). https://doi.org/10.1007/s10967-012-1894-8
79. K. Liu, Z.-F. Chai, W.-Q. Shi, Liquid electrodes for An/Ln separation in pyroprocessing. J. Electrochem. Soc. **168**, 032507 (2021). https://doi.org/10.1149/1945-7111/abec99
80. K. Liu, T. Tan, X. Zhou, N. Zheng, Y. Ma, M. Kang, B. Wang, Z. Chai, W. Shi, The dendrite growth, morphology control and deposition properties of uranium electrorefining. J. Nucl. Mater. **555**, 153110 (2021). https://doi.org/10.1016/j.jnucmat.2021.153110
81. Y. Sakamura, T. Murakami, K. Tada, S. Kitawaki, Electrowinning of U-Pu onto inert solid cathode in LiCl–KCl eutectic melts containing UCl_3 and $PuCl_3$. J. Nucl. Mater. **502**, 270–275 (2018). https://doi.org/10.1016/j.jnucmat.2018.02.025
82. International Atomic Energy Agency, IAEA safeguards glossary, International Nuclear Verification Series No. 3 (Rev. 1), IAEA, Vienna (2002). http://www-pub.iaea.org/MTCD/publications/PDF/nvs-3-cd/PDF/NVS3_prn.pdf
83. B.B. Cipiti, N. Shoman, Pyroprocessing safeguards approach, In: Embed. Top. Meet.-Adv. Nucl. Nonproliferation Technol. Policy Conf. 2018, ANTPC 2018, (2018), p. 77–80
84. P.L. Lafreniere, D.S. Rappleye, R.O. Hoover, M.F. Simpson, E.D. Blandford, Demonstration of signature-based safeguards for pyroprocessing as applied to electrorefining and the ingot casting process. Nucl. Technol. **189**, 173–185 (2015). https://doi.org/10.13182/NT14-35
85. J. Zhang, Electrochemistry of actinides and fission products in molten salts-data review. J. Nucl. Mater. **447**, 271–284 (2014). https://doi.org/10.1016/j.jnucmat.2013.12.017
86. S.X. Li, M.F. Simpson, Anodic process of electrorefining spent driver fuel in molten LiCl–KCI–UCl_3/Cd system. Miner. Metall. Process **22**, 192–198 (2005). https://doi.org/10.1007/bf03403322
87. K. Kim, Y. Jung, S. Paek, S. Kwon, D. Yoon, J. Shim, D. Ahn, H. Lee, Computational analysis for a molten-salt electrowinner with liquid cadmium cathode. J. Korean Radioact. Waste Soc. **8**, 1–7 (2010)

88. S. Yoon, D. Kang, S. Sohn, J. Park, S. Choi, M. Lee, Reference electrode at molten salt: a comparative analysis of electroceramic membranes. J. Nucl. Fuel Cycle Waste Technol. **18**, 143–155 (2020). https://doi.org/10.7733/jnfcwt.2020.18.2.143
89. C. Zhang, J. Wallace, M.F. Simpson, Electrochemical measurement of high concentrations of UCl_3 and $GdCl_3$ in molten LiCl–KCl eutectic. Electrochim. Acta **290**, 429–439 (2018). https://doi.org/10.1016/j.electacta.2018.08.087
90. D. Yoon, S. Phongikaroon, Electrochemical and thermodynamic properties of UCl_3 in LiCl–KCl eutectic salt system and LiCl–KCl–$GdCl_3$ system. J. Electrochem. Soc. **164**, E217–E225 (2017). https://doi.org/10.1149/2.0411709jes
91. M. Iizuka, T. Inoue, O. Shirai, T. Iwai, Y. Arai, Application of normal pulse voltammetry to on-line monitoring of actinide concentrations in molten salt electrolyte. J. Nucl. Mater. **297**, 43–51 (2001). https://doi.org/10.1016/S0022-3115(01)00597-9
92. M. Gonzalez, A. Burak, M.F. Simpson, S. Guo, Identification, measurement, and mitigation of key impurities in LiCl–Li_2O used for direct electrolytic reduction of UO_2. J. Nucl. Mater. **510**, 513–523 (2018). https://doi.org/10.1016/j.jnucmat.2018.08.020
93. Y. Zhang, H. Yin, S. Zhang, D. Tang, Z. Yuan, T. Yan, W. Zheng, D. Wang, Preparation of CeNi2 intermetallic compound by direct electroreduction of solid CeO_2–2NiO in molten LiCl. J. Rare Earths **30**, 923–927 (2012). https://doi.org/10.1016/S1002-0721(12)60155-0
94. T.B. Joseph, N. Sanil, L. Shakila, K.S. Mohandas, K. Nagarajan, A cyclic voltammetry study of the electrochemical behavior of platinum in oxide-ion rich LiCl melts. Electrochim. Acta **139**, 394–400 (2014). https://doi.org/10.1016/j.electacta.2014.07.025
95. G. Young, T. Sham, Initial assessment of metallurgical interaction of clad/base metal systems, Argonne, IL (United States). (2018). https://doi.org/10.2172/1506992
96. C.G. Kontoyannis, Pyrolytic boron nitride coated graphite as a container of reference electrodes for molten fluorides. Electrochim. Acta **40**, 2547–2551 (1995). https://doi.org/10.1016/0013-4686(94)00364-7
97. B.H. Park, I.W. Lee, C.S. Seo, Electrolytic reduction behavior of U_3O_8 in a molten LiCl–Li_2O salt. Chem. Eng. Sci. **63**, 3485–3492 (2008). https://doi.org/10.1016/j.ces.2008.04.021
98. K. Liu, Y.-L. Liu, Z.-F. Chai, W.-Q. Shi, Evaluation of the electroextractions of Ce and Nd from LiCl–KCl Molten salt using liquid Ga electrode. J. Electrochem. Soc. **164**, D169–D178 (2017). https://doi.org/10.1149/2.0511704jes
99. P. Souček, L. Cassayre, R. Malmbeck, E. Mendes, R. Jardin, J.P. Glatz, Electrorefining of U-Pu-Zr-alloy fuel onto solid aluminium cathodes in molten LiCl–KCl. Radiochim. Acta **96**, 315–322 (2008). https://doi.org/10.1524/ract.2008.1493
100. Y. Castrillejo, P. Fernández, J. Medina, P. Hernández, E. Barrado, Electrochemical extraction of samarium from molten chlorides in pyrochemical processes. Electrochim. Acta **56**, 8638–8644 (2011). https://doi.org/10.1016/j.electacta.2011.07.059
101. J.M. Hur, S.M. Jeong, H. Lee, Underpotential deposition of Li in a molten LiCl-Li_2O electrolyte for the electrochemical reduction of U from uranium oxides. Electrochem. Commun. **12**, 706–709 (2010). https://doi.org/10.1016/j.elecom.2010.03.012
102. Y. Sakamura, M. Kurata, T. Inoue, Electrochemical reduction of UO_2 in molten $CaCl_2$ or LiCl. J. Electrochem. Soc. **153**, D31 (2006). https://doi.org/10.1149/1.2160430
103. B.F. Hitch, C.F. Baes, A NiNiO reference electrode of the third kind for molten fluorides. J. Inorg. Nucl. Chem. **34**, 163–169 (1972). https://doi.org/10.1016/0022-1902(72)80374-9
104. M. Shi, S. Li, H. Zhao, High current efficiency of NiO electroreduction in molten salt. J. Electrochem. Soc. **165**, E768–E772 (2018). https://doi.org/10.1149/2.0781814jes
105. R.O. Hoover, M.R. Shaltry, S. Martin, K. Sridharan, S. Phongikaroon, Electrochemical studies and analysis of 1–10 wt% UCl3 concentrations in molten LiCl–KCl eutectic. J. Nucl. Mater. **452**, 389–396 (2014). https://doi.org/10.1016/j.jnucmat.2014.05.057
106. R.L. Hervig, A. Navrotsky, Thermochemistry of sodium borosilicate glasses. J. Am. Ceram. Soc. **68**, 314–319 (1985). https://doi.org/10.1111/j.1151-2916.1985.tb15232.x
107. W. Yang, N. Lee, C. Jung, T.-H. Park, S. Choi, S.-E. Bae, Microelectrode voltammetric analysis of samarium ions in LiCl–KCl eutectic molten salt. Electrochem. Commun. **149**, 107470 (2023). https://doi.org/10.1016/j.elecom.2023.107470
108. D.K. Corrigan, E.O. Blair, J.G. Terry, A.J. Walton, A.R. Mount, Enhanced electroanalysis in lithium potassium eutectic (LKE) using microfabricated square microelectrodes. Anal. Chem. **86**, 11342–11348 (2014). https://doi.org/10.1021/ac5030842
109. R.H. Knibbs, The measurement of thermal expansion coefficient of tungsten at elevated temperatures. J. Phys. E **2**, 311 (1969). https://doi.org/10.1088/0022-3735/2/6/311
110. D. Rappleye, M.L. Newton, C. Zhang, M.F. Simpson, Electroanalytical measurements of binary-analyte mixtures in molten LiCl–KCl eutectic: uranium(III)- and magnesium(II)-chloride. J. Nucl. Mater. **486**, 369–380 (2017). https://doi.org/10.1016/j.jnucmat.2017.01.047
111. R.G. Compton, Craig E Banks, Understanding voltammetry, Third Edit, World Scientific (2018)
112. J. Ge, B. Cai, F. Zhu, Y. Gao, X. Wang, Q. Chen, M. Wang, S. Jiao, Natural convection in molten salt electrochemistry. J. Phys. Chem. B **127**, 8669–8680 (2023). https://doi.org/10.1021/acs.jpcb.3c03938
113. M. Zhou, A. Gallegos, K. Liu, S. Dai, J. Wu, Insights from machine learning of carbon electrodes for electric double layer capacitors. Carbon N. Y. **157**, 147–152 (2020). https://doi.org/10.1016/j.carbon.2019.08.090
114. S. Yoon, S. Choi, Spectroelectrochemical behavior of Cr, Fe Co, and Ni in LiCl–KCl molten salt for decontaminating radioactive metallic wastes. J. Electrochem. Soc. **168**, 013504 (2021). https://doi.org/10.1149/1945-7111/abdc7e
115. G.L. Fredrickson, G. Cao, P.K. Tripathy, M.R. Shaltry, S.D. Herrmann, T.-S. Yoo, T.Y. Karlsson, D.C. Horvath, R. Gakhar, A.N. Williams, R.O. Hoover, W.C. Phillips, K.C. Marsden, Review—electrochemical measurements in molten salt systems: a guide and perspective. J. Electrochem. Soc. **166**, D645–D659 (2019). https://doi.org/10.1149/2.0991913jes
116. T. Tao, J. Wen, Y. Li, C. Ji, J. Wang, W. Sun, The impact of sampling frequency on chemical process monitoring. Comput. Aided Chem. Eng. **49**, 1435–1440 (2022). https://doi.org/10.1016/B978-0-323-85159-6.50239-6
117. J. Wang, A. Ibáñez, M.P. Chatrathi, On-chip integration of enzyme and immunoassays: simultaneous measurements of insulin and glucose. J. Am. Chem. Soc. **125**, 8444–8445 (2003). https://doi.org/10.1021/ja036067e
118. J. Wang, X. Zhang, Needle-type dual microsensor for the simultaneous monitoring of glucose and insulin. Anal. Chem. **73**, 844–847 (2001). https://doi.org/10.1021/ac0009393
119. J.M. Palacios-Santander, L.M. Cubillana-Aguilera, M. Cocchi, A. Ulrici, I. Naranjo-Rodríguez, R. Seeber, J.L. Hidalgo-Hidalgo de Cisneros, Multicomponent analysis in the wavelet domain of highly overlapped electrochemical signals: resolution of quaternary mixtures of chlorophenols using a peg-modified sonogel-carbon electrode. Chemom. Intell. Lab. Syst. **91**, 110–120 (2008). https://doi.org/10.1016/j.chemolab.2007.10.004
120. E.O. Blair, D.K. Corrigan, J.G. Terry, A.R. Mount, A.J. Walton, Development and optimization of durable microelectrodes for quantitative electroanalysis in molten salt. J. Microelectromechanical Syst. **24**, 1346–1354 (2015). https://doi.org/10.1109/JMEMS.2015.2399106

121. C. Pereira, K. Nichols, Testing of a microfluidic sampling system for high temperature prepared for electrochemical MC&A. (2013)
122. Y. Zhao, H. Zhang, Y. Li, X. Yu, Y. Cai, X. Sha, S. Wang, Z. Zhan, J. Xu, L. Liu, AI powered electrochemical multi-component detection of insulin and glucose in serum. Biosens. Bioelectron. **186**, 113291 (2021). https://doi.org/10.1016/j.bios.2021.113291
123. Y. Yoon, M.J. Kim, J.J. Kim, Machine learning to electrochemistry: analysis of polymers and halide ions in a copper electrolyte. Electrochim. Acta **399**, 139424 (2021). https://doi.org/10.1016/j.electacta.2021.139424
124. F. Zhu, J. Ge, Y. Gao, B. Cai, Z. Zhang, F. Jia, S. Jiao, In-situ concentration measurement of soluble-soluble redox couple in molten chlorides utilizing intense natural convection effect. Electrochem. Commun. **155**, 107576 (2023). https://doi.org/10.1016/j.elecom.2023.107576
125. Z. Ballard, C. Brown, A.M. Madni, A. Ozcan, Machine learning and computation-enabled intelligent sensor design. Nat. Mach. Intell. **3**, 556–565 (2021). https://doi.org/10.1038/s42256-021-00360-9
126. International Atomic Energy Agency, Management and storage of research reactor spent nuclear fuel (2009)
127. O. Shirai, H. Yamana, Y. Arai, Electrochemical behavior of actinides and actinide nitrides in LiCl–KCl eutectic melts. J. Alloys Compd. **408–412**, 1267–1273 (2006). https://doi.org/10.1016/j.jallcom.2005.04.119
128. M. Kurata, Y. Sakamura, T. Matsui, Thermodynamic quantities of actinides and rare earth elements in liquid bismuth and cadmium. J. Alloys Compd. **234**, 83–92 (1996). https://doi.org/10.1016/0925-8388(95)01960-X
129. O. Shirai, M. Iizuka, T. Iwai, Y. Arai, Electrode reaction of Pu^{3+}/Pu couple in LiCl–KCl eutectic melts: comparison of the electrode reaction at the surface of liquid Bi with that at a solid Mo electrode. Anal. Sci. **17**, 51–57 (2001). https://doi.org/10.2116/analsci.17.51
130. O. Shirai, K. Uozumi, T. Iwai, Y. Arai, Electrode reaction of the Np^{3+}/Np couple at liquid Cd and Bi electrodes in LiCl–KCl eutectic melts. J. Appl. Electrochem. **34**, 323–330 (2004). https://doi.org/10.1023/B:JACH.0000015615.17281.51
131. O. Shirai, T. Iwai, Y. Suzuki, Y. Sakamura, H. Tanaka, Electrochemical behavior of actinide ions in LiCl–KCl eutectic melts. J. Alloys Compd. **271–273**, 685–688 (1998). https://doi.org/10.1016/S0925-8388(98)00187-X
132. P. Masset, R.J.M. Konings, R. Malmbeck, J. Serp, J.-P. Glatz, Thermochemical properties of lanthanides (Ln=La, Nd) and actinides (An=U, Np, Pu, Am) in the molten LiCl–KCl eutectic. J. Nucl. Mater. **344**, 173–179 (2005). https://doi.org/10.1016/j.jnucmat.2005.04.038
133. P. Masset, D. Bottomley, R. Konings, R. Malmbeck, A. Rodrigues, J. Serp, J.-P. Glatz, Electrochemistry of uranium in molten LiCl–KCl eutectic. J. Electrochem. Soc. **152**, A1109 (2005). https://doi.org/10.1149/1.1901083
134. S.A. Kuznetsov, H. Hayashi, K. Minato, M. Gaune-Escard, Electrochemical behavior and some thermodynamic properties of UCl_4 and UCl_3 dissolved in a LiCl–KCl eutectic melt. J. Electrochem. Soc. **152**, C203 (2005). https://doi.org/10.1149/1.1864532
135. B.P. Reddy, S. Vandarkuzhali, T. Subramanian, P. Venkatesh, Electrochemical studies on the redox mechanism of uranium chloride in molten LiCl–KCl eutectic. Electrochim. Acta **49**, 2471–2478 (2004). https://doi.org/10.1016/j.electacta.2004.02.002
136. F. Gao, C. Wang, L. Liu, J. Guo, S. Chang, L. Chang, R. Li, Y. Ouyang, Electrode processes of uranium ions and electrodeposition of uranium in molten LiCl–KCl. J. Radioanal. Nucl. Chem. **280**, 207–218 (2009). https://doi.org/10.1007/s10967-008-7417-y
137. J. Serp, R.J.M. Konings, R. Malmbeck, J. Rebizant, C. Scheppler, J.P. Glatz, Electrochemical behaviour of plutonium ion in LiCl–KCl eutectic melts. J. Electroanal. Chem. **561**, 143–148 (2004). https://doi.org/10.1016/j.jelechem.2003.07.027
138. H. Shibata, H. Hayashi, T. Koyama, Evaluation of apparent standard potentials of curium in LiCl–KCl eutectic melt. Electrochemistry **83**, 532–536 (2015). https://doi.org/10.5796/electrochemistry.83.532
139. A. Osipenko, A. Maershin, V. Smolenski, A. Novoselova, M. Kormilitsyn, A. Bychkov, Electrochemical behaviour of curium(III) ions in fused 3LiCl–2KCl eutectic. J. Electroanal. Chem. **651**, 67–71 (2011). https://doi.org/10.1016/j.jelechem.2010.10.027
140. Z. Chen, Y.J. Li, S.J. Li, Electrochemical behavior of zirconium in the LiCl–KCl molten salt at Mo electrode. J. Alloys Compd. **509**, 5958–5961 (2011). https://doi.org/10.1016/j.jallcom.2010.10.048
141. R.O. Hoover, D. Yoon, S. Phongikaroon, Effects of temperature, concentration, and uranium chloride mixture on zirconium electrochemical studies in LiCl–KCl eutectic salt. J. Nucl. Mater. **476**, 179–187 (2016). https://doi.org/10.1016/j.jnucmat.2016.04.037
142. L. Xu, Y. Xiao, Q. Xu, Q. Song, Y. Yang, Electrochemistry of zirconium in molten chlorides. Int. J. Electrochem. Sci. **12**, 6393–6403 (2017). https://doi.org/10.20964/2017.07.51
143. S. Li, Y. Che, J. Song, C. Li, Y. Shu, J. He, B. Yang, Electrochemical studies on the redox behavior of Zr(IV) in the LiCl–KCl eutectic molten salt and separation of Zr and Hf. J. Electrochem. Soc. **167**, 023502 (2020). https://doi.org/10.1149/1945-7111/ab69f3
144. J. Park, S. Choi, S. Sohn, K.-R. Kim, I.S. Hwang, Cyclic voltammetry on zirconium redox reactions in LiCl–KCl–$ZrCl_4$ at 500 °C for electrorefining contaminated zircaloy-4 cladding. J. Electrochem. Soc. **161**, H97–H104 (2014). https://doi.org/10.1149/2.046403jes
145. Y. Sakamura, Zirconium behavior in molten LiCl–KCl eutectic. J. Electrochem. Soc. **151**, C187 (2004). https://doi.org/10.1149/1.1644605
146. C.P. Fabian, V. Luca, T.H. Le, A.M. Bond, P. Chamelot, L. Massot, C. Caravaca, T.L. Hanley, G.R. Lumpkin, Cyclic voltammetric experiment -simulation comparisons of the complex mechanism associated with electrochemical reduction of Zr^{4+} in LiCl–KCl eutectic molten salt. J. Electrochem. Soc. **160**, H81–H86 (2013). https://doi.org/10.1149/2.016302jes
147. H. Tang, B. Pesic, Electrochemical behavior of LaCl3 and morphology of la deposit on molybdenum substrate in molten LiCl–KCl eutectic salt. Electrochim. Acta **119**, 120–130 (2014). https://doi.org/10.1016/j.electacta.2013.11.148
148. F. Lantelme, Y. Berghoute, Electrochemical studies of $LaCl_3$ and $GdCl_3$ dissolved in fused LiCl–KCl. J. Electrochem. Soc. **146**, 4137–4144 (1999). https://doi.org/10.1149/1.1392604
149. Y. Wang, W. Zhou, J. Zhang, Investigation of concentration-dependence of thermodynamic properties of lanthanum, yttrium, scandium and terbium in eutectic LiCl–KCl molten salt. J. Nucl. Mater. **478**, 61–73 (2016). https://doi.org/10.1016/j.jnucmat.2016.05.043
150. M. Matsumiya, S.I. Matsumoto, Electrochemical studies on lanthanum ions in molten LiCl–KCl-eutectic mixture. Z. Naturforsch. A. **59**, 711–714 (2004). https://doi.org/10.1515/zna-2004-1015
151. D.K. Sahoo, A.K. Satpati, N. Krishnamurthy, Electrochemical properties of Ce(III) in an equimolar mixture of LiCl–KCl and NaCl–KCl molten salts. RSC Adv. **5**, 33163–33170 (2015). https://doi.org/10.1039/C4RA15334K

152. C. Wang, Y. Liu, H. Hi, F. Gao, L. Liu, S. Chang, J. Guo, L. Chang, Y. Ouyang, Electrochemical behavior of cerium ion in molten LiCl–KCl. J. Rare Earths **31**, 405–409 (2013). https://doi.org/10.1016/S1002-0721(12)60295-6
153. S. Vandarkuzhali, M. Chandra, S. Ghosh, N. Samanta, S. Nedumaran, B. Prabhakara Reddy, K. Nagarajan, Investigation on the electrochemical behavior of neodymium chloride at W, Al and Cd electrodes in molten LiCl–KCl eutectic. Electrochim. Acta **145**, 86–98 (2014). https://doi.org/10.1016/j.electacta.2014.08.069
154. S.E. Bae, T.S. Jung, Y.H. Cho, J.Y. Kim, K. Kwak, T.H. Park, Electrochemical formation of divalent samarium cation and its characteristics in LiCl–KCl melt. Inorg. Chem. **57**, 8299–8306 (2018). https://doi.org/10.1021/acs.inorgchem.8b00909